

Non-Gaussian enhancement of precision in quantum batteries

Beatriz Polo^{1,*} and Federico Centrone^{1,2,†}

¹*ICFO-Institut de Ciències Fòtoniques, The Barcelona Institute of Science and Technology, Av. Carl Friedrich Gauss 3, 08860 Castelldefels (Barcelona), Spain.*

²*Universidad de Buenos Aires, Instituto de Física de Buenos Aires (IFIBA), CONICET, Ciudad Universitaria, 1428 Buenos Aires, Argentina.*

We investigate the fundamental limits of converting light into useful work, with a focus on the role of quantum resources in energy harvesting processes. Specifically, we analyze how quantum coherence, non-Gaussianity, and entanglement affect the fluctuations in the energy output of bosonic quantum batteries. Our findings reveal potential pathways to enhance the efficiency and stability of energy extraction from quantum batteries, with implications for the development of quantum thermal machines at the nanoscale. Moreover, this work highlights a tangible thermodynamic quantum advantage, demonstrating how quantum effects can be harnessed to improve the performance of practical energy conversion tasks.

Introduction.—While originally motivated by the industrial necessity of optimizing engine performance, thermodynamics produced some of science’s deepest and most interconnected concepts, ranging from cosmology to information theory to biology [1]. Quantum thermodynamics [2] has the potential to share the same success as its classical counterparts, in a moment where energetic optimization is a fundamental demand and where quantum technologies are receiving notable attention [3]. Quantum batteries are one of the most trending topics in the community [4–8], demonstrating the promise of an energetic quantum advantage in terms of charging power. While being a concept of fundamental interest, power is not a significant figure of merit for practical scenarios, because of the low energetic scales of quantum systems and the resources required to prepare them [9]. In addition, while having characterized the many ways quantum systems can store work, studies about the practical extraction and usage of such energy are limited [10].

The edge of quantum mechanics was never about large energies, as proposed by the recent literature on quantum batteries, but about precision, as demonstrated by quantum metrological experiments [11–13]. Precision is also one of the prominent topics of thermodynamics ever since its statistical formulation. In a future fueled by quantum technologies, it is thus hard to imagine that an array of cold atoms will allow the powerful charging of a laptop or anything similar. However, to supply power to the emerging nanotechnologies, realistically, it will be necessary to take into account quantum fluctuations [14]. Such devices require an exact amount of energy to produce useful work, and classical fluctuations risk either destroying them or not charging them at all [15]. Nanobots are typically charged with external power sources to maintain their movement autonomy, using light pulses, magnetic fields, or acoustic waves [16–18]. The natural language to describe this dynamic in the quantum setting is the continuous variables formalism [19]. In the following, we will adopt a quantum optics nomenclature, however, our framework can be easily translated to describe any bosonic quantum field, such as phonons.

In this manuscript, we show new fundamental findings as a means to practical applications for efficient energy processing. The task we propose, precision energy extraction from quantum light, naturally imposes a hierarchy on the type of operations we can perform, enabling the possibility of demonstrating a quantum advantage in terms of a thermodynamic quantity using entangling non-Gaussian unitaries. We optimize quantum batteries under realistic experimental constraints to maximize the signal-to-noise ratio of the work conversion from an energy harvester. Moreover, our scheme is readily implementable in a well-equipped quantum photonics laboratory.

Bosonic batteries.— A quantum battery is defined as a system whose internal Hamiltonian H_0 has non-degenerate energy levels¹, such that energy can be temporarily stored by performing unitary operations U on an initial thermal state ρ_0 to prepare the system in some excited state $\rho = U\rho_0U^\dagger$. The energy stored in the battery during this process will afterwards act as the external source for some other device, referred to in this work as *energy harvester*, capable of transforming the battery’s potential into useful work (e.g. to power some nanotechnological task [20–22]). In the following, we will assume the battery to be a free propagating electromagnetic field (i.e., a light pulse), however, the same analysis works for any oscillatory system, such as harmonic excitations in crystals.

As for the energy harvester, examples of these kinds of devices include photo-diodes, piezoelectric crystals, or quantum dots [23]. To maintain the discussion on a general level, we will omit the technicalities of a specific system and assume that this device is anything that generates an electrical current proportional to the number of excitations of the external field $N = \sum_i a_i^\dagger a_i$, where we are using the notation of bosonic ladder operators, and we are discretizing the field frequencies to simplify the

¹ In fact, a more relaxed condition of a partially degenerated spectrum, i.e. such that the eigenvalues satisfy the relation $\epsilon_k \leq \epsilon_{k+1}$ as long as the bandwidth $\epsilon_{\max} - \epsilon_{\min}$ is non-zero, is sufficient for the definition of a quantum battery [4].

analysis. The mean electrical current at the output will be given by the product of the mean number of photons $\langle N \rangle$, the repetition rate of the laser source f , and a constant that characterizes the efficiency of the process μ . The scheme is synthesized in figure 1. The study of a more realistic model, where the current depends on the continuous envelope of the frequency, will be the subject of future studies.

In the following, we can thus focus on optimizing the charging protocol of the battery to arrive at a state with minimal fluctuations of the photon number $\Delta^2 N = \langle N^2 \rangle - \langle N \rangle^2$. Initially at $t < 0$, the optical field constituting the battery will be in a thermal passive state at temperature T for the free harmonic oscillator Hamiltonian $H_0 = \sum_i \omega_i (n_i + \frac{1}{2})$, characterized by a density matrix $\rho_0 = \frac{e^{-H_0/k_B T}}{\text{Tr}[e^{-H_0/k_B T}]}$, producing a background thermal current on the harvester proportional to

$$N_0 = \text{Tr}[N\rho_0]. \quad (1)$$

For $t > 0$ the quantum state of light evolves according to the Hamiltonian $H = H_0 + V(t)$, where the time-dependent potential $V(t)$ is used to change the number of photons to charge the battery. For simplicity, we will assume a constant potential that is instantaneously turned on at the beginning of the protocol and turned off at the end $V(0) = V(\tau) = 0$. The difference between the initial and final current produced by the harvester will thus be proportional to

$$\delta N = \text{Tr}[N(\rho - \rho_0)], \quad (2)$$

where the unitary $U = e^{iV\tau/\hbar}$ and $\rho = U\rho_0U^\dagger$. The fluctuations of this current are given by

$$\Delta N = \sqrt{\text{Tr}[N^2\rho] - (\text{Tr}[N\rho])^2}. \quad (3)$$

We assume that the potential V can be written as a polynomial of the ladder operators. The degree of this polynomial dramatically changes the type of states that can be produced and will limit the type of fluctuation generated in the electrical current of the harvester. Namely, in the first order, we have classical fields such as coherent states; in the second order, we have quantum squeezed states, which can suppress the fluctuations associated with certain observables [24, 25]. With more than quadratic potentials, we can generate non-Gaussian states that play a prominent role in different areas of quantum information [26]. We will show that these states are fundamental to achieving arbitrary precisions in energy harvesting and unlocking the advantage of entangling operations.

In line with this motivation, the figure-of-merit Γ that we will seek to maximize will take the form of a *signal-to-noise* ratio (SNR), between the mean number of photons injected into the battery through the charging process, δN , and its uncertainty:

$$\Gamma = \frac{\delta N}{\Delta N}. \quad (4)$$

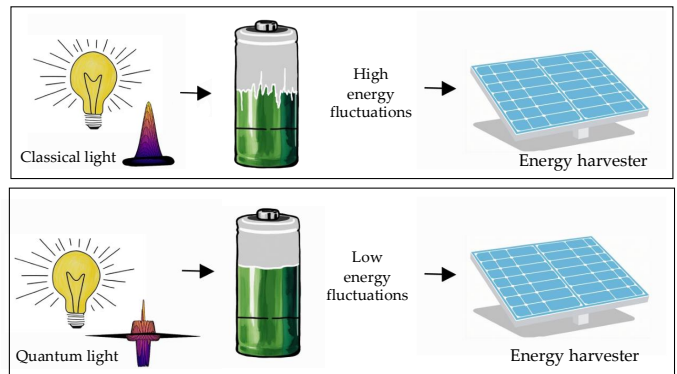


FIG. 1: Scheme of the charging precision in a photonic-based battery. Energy fluctuations are attenuated when employing non-classical light.

Being interested in the more realistic scenario where energy inputs are limited, we fix the maximum allowed δN at some value ϵ .

The *signal-to-noise* ratio Γ is related to the second-order intensity correlation function $g^{(2)}(0)$, which is a measure of temporal photon coincidences [27]

$$g^{(2)}(0) = \left(\Gamma + \frac{N_0}{\Delta N} \right)^{-2} - \frac{1}{\langle N \rangle} + 1. \quad (5)$$

A value of $g^{(2)}(0)$ smaller than unity is a necessary and sufficient condition for the identification of quantum states of light undergoing the phenomenon of antibunching [28]. Using Eq.5, this criterion for antibunching can be equivalently rewritten as:

$$\left(\Gamma + \frac{N_0}{\Delta N} \right)^2 > \langle N \rangle \iff \text{antibunching} \quad (6)$$

Depending on whether the mean photon number of a light source is smaller, equal or greater than its squared variance, their distributions are referred to as super-Poissonian, Poissonian, or sub-Poissonian, respectively. Both Poissonian and super-Poissonian light can be described by a semi-classical theory, in which the light source is modeled as an electromagnetic wave. In contrast, sub-Poissonian light sources are non-classical and are preferable in various applications. They exhibit lower photon-number fluctuations, which is advantageous in high-precision measurements and information processing tasks where minimization of the noise plays a significant role [29, 30].

Gaussian limitations.— States that can be engineered through Gaussian unitary operations have many desirable properties. They are easy to implement with a high degree of experimental control in state-of-the-art quantum photonics hardware [31, 32]. From a theoretical perspective, the properties and dynamics of Gaussian states can be efficiently simulated with a classical computer. Although these states are infinite-dimensional, they allow for a simple mathematical description through symplec-

tic geometry. Despite their relevance from both a fundamental and practical point of view, Gaussian unitaries are limited. In particular, in the context of quantum batteries, we show that they are suboptimal resources for the charging process. For the sake of simplicity, we will initially restrict to the single-mode scenario, in which the initial constraint ϵ on the battery's maximum mean photon number reads $\delta N \leq \epsilon$. The generalization to multiple modes is discussed at the end of the Supplementary Material (SM).

The harvested energy *signal-to-noise* ratio of a single-mode Gaussian state ρ reads:

$$\Gamma(\rho) = \frac{N(\rho) - N(\rho_0)}{\Delta N(\rho)} = \frac{\frac{1}{4}(\text{Tr}(\sigma) - 2) + \|\alpha\|^2 - N(\rho_0)}{\sqrt{\alpha^T \sigma \alpha + \frac{1}{8}[\text{Tr}(\sigma^2) - 2]}} \quad (7)$$

where $\alpha = (\alpha_1, \alpha_2)^T = \frac{1}{\sqrt{2}}(\langle x \rangle, \langle p \rangle)^T$ is the vector of displacements, σ is the covariance matrix of state ρ , and ρ_0 is the passive thermal state associated to ρ , whose energy is a constant term N_0 only dependent on its thermal fluctuations parameter ν :

$$N_0 = \frac{1}{2}(\nu - 1) \quad \text{with} \quad \nu = \coth\left(\frac{\omega}{k_B T}\right) \quad (8)$$

The explicit expressions for the numerator and denominator of the quotient in Eq.7 read:

$$N(\rho) - N(\rho_0) = \frac{1}{4}\nu\left(z + \frac{1}{z} - 2\right) + \|\alpha\|^2 \quad (9)$$

$$\Delta N = \sqrt{\frac{1}{8}\nu^2\left(z^2 + \frac{1}{z^2}\right) - \frac{1}{4} + \nu\left(\alpha_1^2 z + \alpha_2^2 \frac{1}{z}\right)} \quad (10)$$

Note that given a certain fluctuation degree of our system ν , the ratio Γ of any Gaussian state is determined by the squeezing and displacement transformations applied (parametrized by z and α , respectively), showing no phase dependence.

Let us first consider coherent states, a specific case of Gaussian states that are present in many experimental realizations due to their ease of generation and manipulation. These are the states that most closely resemble the classical wave-like behavior, exhibiting super-Poissonian or Poissonian distributions with $g^{(2)}(0) \geq 1$ (with equality only in the pure case), which cannot display the phenomenon of antibunching. This limitation of coherent states can also be manifest by computing our figure of merit Γ upon the substitution $z = 1$ (no squeezing is applied, just displacement transformations are performed).

$$\Gamma(\rho_{\text{coherent}}) = \frac{\|\alpha\|^2}{\sqrt{\frac{1}{4}(\nu^2 - 1) + \nu\|\alpha\|^2}}, \quad (11)$$

The condition $\|\alpha\|^2 = \delta N \leq \epsilon$ implies that the *signal-to-noise* ratio for coherent states must be bounded:

$$\Gamma(\rho_{\text{coherent}}) \leq \|\alpha\| \leq \sqrt{\epsilon} \quad (12)$$

As a consequence, introducing a higher degree of non-classicality is essential to obtain better precision performances in the charging protocol.

Remaining within the Gaussian realm, we now consider the application of quadrature squeezing z to an initial thermal state. Squeezing is an inherently quantum resource that can result in Gaussian states exhibiting sub-Poissonian statistics ($g^{(2)}(0) < 1$). In the context of quantum batteries [33], if a vacuum or thermal state undergoes squeezing transformations only, its *signal-to-noise* ratio will again be upper-bounded:

$$\Gamma(\rho_{\text{squeezed}}) \leq 1 \quad (13)$$

since

$$\frac{1}{4}\nu\left(z + \frac{1}{z} - 2\right) \leq \underbrace{\sqrt{\frac{1}{8}\nu^2\left(z^2 + \frac{1}{z^2}\right) - \frac{1}{4}}}_{\Delta N} \quad \forall z \in (0, 1] \quad (14)$$

Squeezed-only batteries perform worse than coherent states if the state contains more than one photon. The optimal Gaussian Γ at a certain temperature and given some fixed ergotropy constraint ϵ will thus be obtained by a combination of both displacement and squeezing such that the energy uncertainty in the resulting state is minimized. The solution to this optimization problem is obtained through the method of Lagrange multipliers, and further discussed in the SM. In Figure 2 the optimal Gaussian ratio is plotted for a range of temperatures and ergotropy constraint values. We observe that by combin-

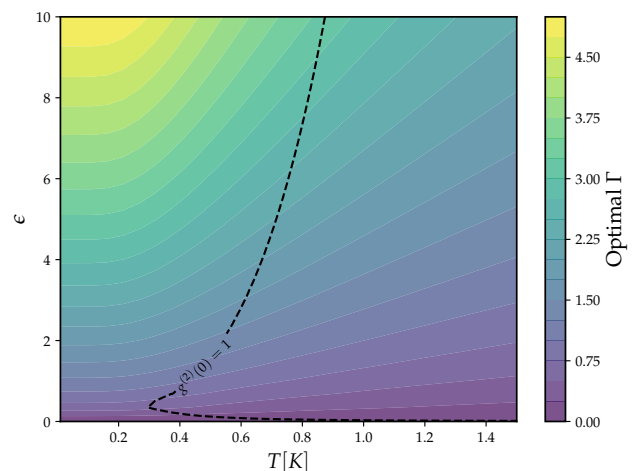


FIG. 2: Maximum photon number SNR attainable for Gaussian states as a function of temperature and the maximum energy input allowed in the device.

ing squeezing and displacement, one can overcome the classical bounds in Eqs. 12, 13, encountered when these operations are performed individually. In fact, for highly squeezed batteries (which appear to be optimal in most cases), we find that the maximum Gaussian ratio can be

approximated by the following analytical expression:

$$\Gamma_{opt} \approx \frac{8\epsilon}{\nu^2 \left[3 \left(\frac{4\epsilon}{\nu} + 2 \right)^{\frac{2}{3}} - 2 + \left(\frac{4\epsilon}{\nu} + 2 \right)^{\frac{-2}{3}} \right]} \quad (15)$$

The dashed line in the figure represents the boundary $g^{(2)}(0) = 1$ between super- and sub-Poissonian photon number distribution of the light source, that is, between classical and quantum behaviour. Note that, since coherent states have super-Poissonian distributions, the acquisition of sub-Poissonian statistics in the optimal states is due to the application of quadrature squeezing. This shows that the energetic signal-to-noise ratio Γ is a witness of non-classicality. We now turn to the exploration of a broader set of CV states, which can provide a significant improvement in performance.

Non-Gaussian states. – At zero temperature, the simplest non-Gaussian state, namely the Fock state $|n\rangle$, has a perfectly well-defined expectation value n of the photon number observable with zero variance, therefore yielding $\Gamma \rightarrow \infty$ and becoming the optimal battery. However, as is highlighted in Fig.3, the situation changes dramatically in realistic scenarios. Subject to thermal fluctuations, the uncertainty in the mean photon number of thermal Fock states increases more rapidly than that of squeezed states, which are more robust to temperature increases. Consequently, a thermal regime exists where Fock states no longer provide a significant advantage in the *signal-to-noise* ratio compared to the Gaussian case, and it thus becomes necessary to explore alternative protocols for precise energy extraction. In [34],

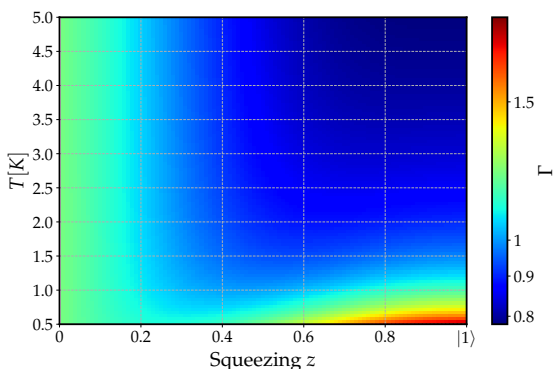


FIG. 3: SNR of a photon-added squeezed thermal state as a function of thermal fluctuations and squeezing. The pure Fock state $|1\rangle$ corresponds to no squeezing ($z = 1$) and zero temperature.

an abstract mathematical construction of bosonic states with minimal variance is described and compared to the optimal Gaussian performance. Here we propose an explicit, physically-inspired ansatz for the construction of non-Gaussian states, namely those with the form of a Gaussian plus successive creation operations:

$$\rho_{NG} = (a_1^\dagger)^m \underbrace{U_G \rho_0 U_G^\dagger}_{\rho_G} (a_1)^m \quad (16)$$

States engineered following this prescription can be realized experimentally in a photonic setup [35] through consecutive application of ladder operators (addition or subtraction). Moreover, all bosonic unitaries can be developed in a power series of ladder operators, and in certain cases, it also allows for resummation of an infinite series (see the cat state example in SM). Hence, this ansatz not only allows us to describe practical non-Gaussian states, but, with small adaptations, it potentially encompasses all states of an infinite-dimensional Hilbert space. In addition, the statistical moments of this kind of state allow for exact calculation by applying Wick's theorem [36]. By using a variational algorithm [37], we find optimal values of the Gaussian unitary U_G to maximize the SNR.

In Fig.4 we show the dependence on temperature of the highest ratio that can be attained for a different number of ladder operations, after optimal tuning of the Gaussian block's U_G parameters. In addition, the behavior of Γ is also shown for the superposition of a coherent and a Fock (with $n = 5$) state in contact with a thermal bath at temperature T , whose photon-number statistical moments are derived in [38], and a noisy *kitten* state, modeled as a photon-subtracted squeezed thermal state, as suggested in [39, 40]. The analytics for the calculation of Γ for the kitten states can be found in the SM.

Different kinds of non-Gaussian states can violate the Gaussian bound (black dashed line). Photon-added states become Fock states at zero temperature, and the SNR explodes as their fluctuations vanish. Noisy cat states showcase a similar behaviour, although their advantage with respect to the Gaussian bound is more sensitive to fluctuations than it is for photon-added states. On the contrary, coherent-Fock thermal states appear to be more noise-robust and display more stable *signal-to-noise* ratios, violating the Gaussian bound in the low thermal fluctuations regime. We also observe that photon-added states are more resilient to noise if we increase the number of photon additions. The intersections of the solid lines in Fig.4 with the Gaussian bound indicate the temperatures at which one more photon addition is needed to overcome the best Gaussian ratio. Whether these photon-added states can be considered as potential candidates for the charging process or not depends on the value of the mean photon number constraint ϵ imposed by each specific use case. A detailed discussion on the conditions for feasibility is provided in the SM.

Conclusion. – In this work, we describe the performance of bosonic quantum batteries under realistic physical constraints. We introduce a new figure of merit, the SNR of the energy conversion, that is practically motivated by the precision charging of nano-scale energy harvesters. This figure of merit naturally introduces a hierarchy of the type of states used as batteries. We find optimal values of the experimental parameters required to implement the batteries that minimize the fluctuations of the energy conversion. We find connections between the SNR and other relevant quantities in quantum optics and

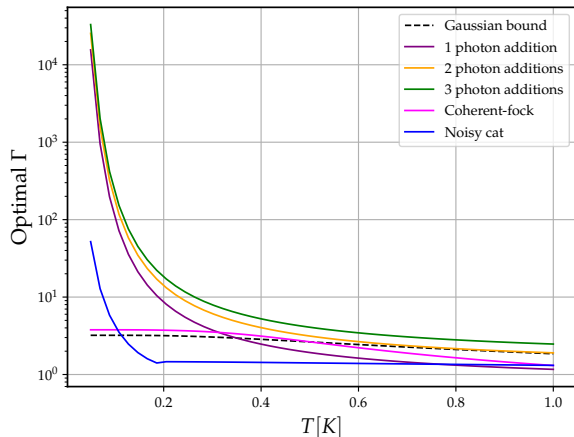


FIG. 4: Optimal Γ attainable for zero (Gaussian) to three photon-added states, thermal-Fock and noisy cat states, as a function of temperature. The constraint has been set at $\epsilon = 5$ (dimensionless).

quantum information and use them to show that it can be an indicator of non-classicality and non-Gaussianity. Furthermore, we provide evidence of the potential gain in SNR through the application of entangling operations in the non-Gaussian realm. We provide analytical calculations to support our findings that can be easily adapted to other physically relevant scenarios. A possible follow-up of this work would be to introduce a more realistic noise model and use quantum control theory to minimize the fluctuations of the batteries dynamically. In addition, our model paves the way to study how non-Gaussianity affects fluctuations in the context of thermodynamic uncertainty relations. The experimental implementation of this protocol would constitute the first demonstration of quantum advantage for a thermodynamic practical scenario, with relevant applications in the miniaturization of nanotechnologies.

Acknowledgements: The authors thank Antonis Delakouras, Manuel Gessner and Francesco Flora for fruitful discussions and inputs, and notably Antonio Acín for his relevant feedback and guidance.

Funded by the European Union (EQC, 101149233), the Government of Spain (Severo Ochoa CEX2019-000910-S), Fundació Cellex, Fundació Mir-Puig, Generalitat de Catalunya (CERCA program). Views and opinions expressed are however, those of the author(s) only and do not necessarily reflect those of the European Union or European Research Executive Agency. Neither the European Union nor the granting authority can be held responsible for them.

* beatriz.polo@icfo.eu

† federico.centrone@icfo.eu.

[1] M. Goldstein and I. F. Goldstein, *The refrigerator and*

the universe: understanding the laws of energy (Harvard University Press, 1995).

- [2] F. Binder, L. A. Correa, C. Gogolin, J. Anders, and G. Adesso, *Fundamental Theories of Physics* **195** (2018).
- [3] A. Auffèves, *PRX Quantum* **3**, 020101 (2022), URL <https://link.aps.org/doi/10.1103/PRXQuantum.3.020101>.
- [4] F. Campaioli, S. Gherardini, J. Q. Quach, M. Polini, and G. M. Andolina, *Rev. Mod. Phys.* **96**, 031001 (2024), URL <https://link.aps.org/doi/10.1103/RevModPhys.96.031001>.
- [5] T. K. Konar, A. Patra, R. Gupta, S. Ghosh, and A. Sen(De), *Physical Review A* **110** (2024), ISSN 2469-9934, URL <http://dx.doi.org/10.1103/PhysRevA.110.022226>.
- [6] J. Quach, G. Cerullo, and T. Virgili, *Joule* **7**, 2195 (2023), ISSN 2542-4351, URL <https://www.sciencedirect.com/science/article/pii/S2542435123003641>.
- [7] A. Camposeo, T. Virgili, F. Lombardi, G. Cerullo, D. Pisignano, and M. Polini, *Advanced Materials* **37** (2025), ISSN 1521-4095, URL <http://dx.doi.org/10.1002/adma.202415073>.
- [8] H.-L. Shi, L. Gan, K. Zhang, X.-H. Wang, and W.-L. Yang, *Quantum charging advantage from multipartite entanglement* (2025), 2503.02667, URL <https://arxiv.org/abs/2503.02667>.
- [9] Y. Kurman, K. Hymas, A. Fedorov, W. J. Munro, and J. Quach, *Quantum computation with quantum batteries* (2025), 2503.23610, URL <https://arxiv.org/abs/2503.23610>.
- [10] N. M. Myers, O. Abah, and S. Deffner, *AVS Quantum Science* **4** (2022), ISSN 2639-0213, URL <http://dx.doi.org/10.1116/5.0083192>.
- [11] R. Liu, Y. Chen, M. Jiang, X. Yang, Z. Wu, Y. Li, H. Yuan, X. Peng, and J. Du, *npj Quantum Information* **7** (2021), ISSN 2056-6387, URL <http://dx.doi.org/10.1038/s41534-021-00507-x>.
- [12] P. Yin, X. Zhao, Y. Yang, Y. Guo, W.-H. Zhang, G.-C. Li, Y.-J. Han, B.-H. Liu, J.-S. Xu, G. Chiribella, et al., *Nature Physics* **19**, 1122 (2023), URL <https://doi.org/10.1038/s41567-023-02046-y>.
- [13] W. Jia, V. Xu, K. Kuns, M. Nakano, L. Barsotti, M. Evans, N. Mavalvala, L. S. Collaboration†, R. Abbott, I. Abouelfettouh, et al., *Science* **385**, 1318 (2024), URL <https://www.science.org/doi/abs/10.1126/science.ad08069>.
- [14] M. LaHaye, O. Buu, B. Camarota, and K. Schwab, *Science* **304**, 74 (2004), URL <https://www.science.org/doi/abs/10.1126/science.1094419>.
- [15] M. Ussia, V. Privitera, and S. Scalese, *Advanced Materials Interfaces* **11**, 2300970 (2024), URL <https://doi.org/10.1002/admi.202300970>.
- [16] K. C. Mishra, *International Journal of Advances in Engineering & Technology* **4**, 564 (2012), URL <https://www.ijaet.org/media/0007/63I10-IJAET1009228-A-REVIEW-ON-SUPPLY.pdf>.
- [17] G. Giri, Y. Maddahi, and K. Zareinia, *Applied Sciences* **11**, 10385 (2021), URL <https://www.mdpi.com/2076-3417/11/21/10385>.
- [18] H. Zhou, C. C. Mayorga-Martinez, S. Pané, L. Zhang, and M. Pumera, *Chemical Reviews* **121**, 4999 (2021), URL <https://doi.org/10.1021/acs.chemrev.0c01234>.
- [19] A. Serafini, *Quantum continuous variables: a primer of theoretical methods* (CRC press, 2023).
- [20] G. Jaliel, R. Puddy, R. Sánchez, A. Jordan, B. Sothmann,

- I. Farrer, J. Griffiths, D. Ritchie, and C. Smith, *Physical review letters* **123**, 117701 (2019), URL <https://link.aps.org/doi/10.1103/PhysRevLett.123.117701>.
- [21] O. Culhane, M. T. Mitchison, and J. Goold, *Physical Review E* **106**, L032104 (2022), URL <https://link.aps.org/doi/10.1103/PhysRevE.106.L032104>.
- [22] F. Meng, J. Xu, X. Liu, and O. Dahlsten, *Phys. Rev. A* **111**, 012219 (2025), URL <https://link.aps.org/doi/10.1103/PhysRevA.111.012219>.
- [23] J. D. Phillips, *Frontiers in Nanotechnology* **3**, 633931 (2021), URL <https://doi.org/10.3389/fnano.2021.633931>.
- [24] T. Ono, J. Sabines-Chesterking, H. Cable, J. L. O'Brien, and J. C. F. Matthews, *New Journal of Physics* **19**, 053005 (2017), ISSN 1367-2630, URL <http://dx.doi.org/10.1088/1367-2630/aa6e39>.
- [25] E. Shchukin, T. Kiesel, and W. Vogel, *Phys. Rev. A* **79**, 043831 (2009), URL <https://link.aps.org/doi/10.1103/PhysRevA.79.043831>.
- [26] M. Walschaers, *PRX Quantum* **2**, 030204 (2021), URL <https://link.aps.org/doi/10.1103/PRXQuantum.2.030204>.
- [27] R. J. Glauber, *Phys. Rev.* **130**, 2529 (1963), URL <https://link.aps.org/doi/10.1103/PhysRev.130.2529>.
- [28] M.-A. Lemonde, N. Didier, and A. A. Clerk, *Phys. Rev. A* **90**, 063824 (2014), URL <https://link.aps.org/doi/10.1103/PhysRevA.90.063824>.
- [29] B.-m. Ann, Y. Song, J. Kim, D. Yang, and K. An, *Scientific Reports* **9** (2019), ISSN 2045-2322, URL <http://dx.doi.org/10.1038/s41598-019-53525-3>.
- [30] I. R. Berchera and I. P. Degiovanni, *Metrologia* **56**, 024001 (2019), ISSN 1681-7575, URL <http://dx.doi.org/10.1088/1681-7575/aaf7b2>.
- [31] J. B. Brask, *Gaussian states and operations – a quick reference* (2022), 2102.05748, URL <https://arxiv.org/abs/2102.05748>.
- [32] M. Zhang, S. Chowdhury, and L. Jiang, *npj Quantum Information* **8** (2022), ISSN 2056-6387, URL <http://dx.doi.org/10.1038/s41534-022-00581-9>.
- [33] F. Centrone, L. Mancino, and M. Paternostro, *Phys. Rev. A* **108**, 052213 (2023), URL <https://link.aps.org/doi/10.1103/PhysRevA.108.052213>.
- [34] N. Friis and M. Huber, *Quantum* **2**, 61 (2018), ISSN 2521-327X, URL <http://dx.doi.org/10.22331/q-2018-04-23-61>.
- [35] G. Roeland, S. Kaali, V. R. Rodriguez, N. Treps, and V. Parigi, *New Journal of Physics* **24**, 043031 (2022), URL [10.1088/1367-2630/ac5f85](https://doi.org/10.1088/1367-2630/ac5f85).
- [36] M. Walschaers, C. Fabre, V. Parigi, and N. Treps, *Phys. Rev. A* **96**, 053835 (2017), URL <https://link.aps.org/doi/10.1103/PhysRevA.96.053835>.
- [37] P. Stornati, A. Acin, U. Chabaud, A. Dauphin, V. Parigi, and F. Centrone, *Variational quantum simulation using non-gaussian continuous-variable systems* (2024), URL <https://link.aps.org/doi/10.1103/PhysRevResearch.6.043212>.
- [38] P. Weber, V. Lula-Rocha, J. Pereira, M. Trindade, L. S. Filho, M. Martins, A. Santana, and J. Vianna, *Annals of Physics* **443**, 168986 (2022), ISSN 0003-4916, URL <https://www.sciencedirect.com/science/article/pii/S0003491622001415>.
- [39] A. Ourjoumtsev, R. Tualle-Brouri, J. Laurat, and P. Grangier, *Science* **312**, 83 (2006), <https://www.science.org/doi/pdf/10.1126/science.1122858>, URL <https://www.science.org/doi/abs/10.1126/science.1122858>.
- [40] K. Wakui, H. Takahashi, A. Furusawa, and M. Sasaki, *Optics Express* **15**, 3568 (2007), ISSN 1094-4087, URL <http://dx.doi.org/10.1364/OE.15.003568>.
- [41] S.-H. Tan and P. P. Rohde, *Reviews in Physics* **4**, 100030 (2019), ISSN 2405-4283, URL <https://www.sciencedirect.com/science/article/pii/S2405428318300431>.
- [42] A. Björklund, B. Gupt, and N. Quesada, *Journal of Experimental Algorithmics (JEA)* **24**, 1 (2018), URL <https://api.semanticscholar.org/CorpusID:141413702>.

Covariance matrix formalism for Gaussian states

Gaussian states can be understood as the set of all ground and thermal states of Hamiltonians that are at most quadratic in the quadrature variables x and p . These quadratures, also referred to as canonical operators, can be chosen to be any pair of operators acting on the system's Hilbert space and satisfying the canonical commutation relations:

$$[x_i, p_j] = i\hbar\delta_{ij} \quad (17)$$

In the harmonic oscillator picture, they are usually represented by the position and momentum of a particle, but when dealing with quantum states of light, it is the real and imaginary components of the electromagnetic field that play the roles of the quadrature variables.

This Gaussian set entails the operational advantage that all of its states have positively-valued normal distributions in phase space, and thus admit a full characterization through the first and second statistical moments of x and p , which are encoded in a vector of displacements, and the so-called covariance matrix, respectively. Knowledge of these two degrees of freedom is thus sufficient to extract any information of interest from a Gaussian state.

There exist various possibilities for the parametrization of a Gaussian state's covariance matrix. For the sake of a greater intuition on the properties of the states on which we are computing the *signal-to-noise* ratio Γ , we will adopt the typical approach used in the context of quantum optics and photonics that describes such matrix in terms of the transformations applied to an initially thermal state in an optical setup. According to Williamson's theorem, the covariance matrix of any Gaussian state can be written as the product:

$$\sigma = S \left(\bigoplus_{j=1}^N \nu_j \mathbb{1}_2 \right) S^T \quad (18)$$

where $S \in Sp_{2n, \mathbb{R}}$ is a symplectic transformation that can also be, through the Bloch-Messiah decomposition theorem, split into:

$$S = O_1 Z O_2 \quad (19)$$

with

$$O_1, O_2 \in O(2N) \cap Sp_{2n, \mathbb{R}} \cong U(N)$$

representing the set of passive optics unitaries, and

$$Z = \bigoplus_{j=1}^N \begin{pmatrix} z_j & 0 \\ 0 & z_j^{-1} \end{pmatrix} \quad z \in (0, 1] \quad (20)$$

a squeezing transformation of parameter z . This representation allows for the interpretation of every Gaussian state as the result of applying a single mode squeezing transformation followed by a linear optical passive setup to an initial thermal (and possibly displaced) state of N modes. Such initial state would have covariance matrix $\sigma_0 = \bigoplus_{j=1}^N \nu_j \mathbb{1}_2$, where the ν_i are referred to as symplectic eigenvalues, and can be understood in this context as fluctuation parameters indicating the temperature T_i that characterizes the initial thermal state of each of the modes through the relation:

$$\nu_i = \coth \left(\frac{\omega_i}{k_B T} \right) \quad (21)$$

The matrices O_1, O_2 represent the energy-preserving *passive optics* transformations, which can be decomposed into beam splitters (semi-reflective mirrors parametrized by their transmissivity $\cos^2 \theta$ that mix up pairs of modes) and phase shifters (dielectric plates that rotate the optical phase of an electromagnetic wave by some angle φ). A scheme of alternating applications of these two operations to create the most general linear interferometer is detailed in [41]. Matrix Z represents local or single-mode squeezing, which, in contrast, is an active operation, requiring energy from an external laser field that pumps a nonlinear crystal through which the optical modes travel. The result of this transformation is a contraction of the variance of one of the canonical variables and the expansion of its conjugate one. Squeezing and beam splitting allow the generation of quantum correlations among different modes of the quantum state.

The most general single-mode Gaussian covariance matrix in terms of the elementary quantum optical operations takes the form:

$$\sigma = \nu \begin{pmatrix} z \cos^2 \varphi + \frac{1}{z} \sin^2 \varphi & \frac{1-z^2}{2z} \sin(2\varphi) \\ \frac{1-z^2}{2z} \sin(2\varphi) & z \sin^2 \varphi + \frac{1}{z} \cos^2 \varphi \end{pmatrix} \quad (22)$$

The mean and variance of the photon number operator can be obtained through (see [34])

$$N(\rho) = \frac{1}{4}(\text{Tr}(\sigma) - 2) + \|\alpha\|^2 \quad (23)$$

$$\Delta N(\rho) = \sqrt{\alpha^T \sigma \alpha + \frac{1}{8}[\text{Tr}(\sigma^2) - 2]} \quad (24)$$

and thus depend, upon substitution of σ as in Eq.22, on the fluctuation parameter ν that accounts for temperature, the squeezing factor $z \in (0, 1]$, the dephasing angle $\varphi \in [0, 2\pi)$ and the displacement vector α :

$$N(\rho) - N(\rho_0) = \frac{1}{4}\nu \left(z + \frac{1}{z} - 2 \right) + \|\alpha\|^2 \quad (25)$$

$$\begin{aligned} (\Delta N(\rho))^2 &= \frac{1}{8}\nu^2 \left(z^2 + \frac{1}{z^2} \right) - \frac{1}{4} \\ &+ \nu \left[\alpha_1^2 \left(z \cos^2 \varphi + \frac{1}{z} \sin^2 \varphi \right) \right. \\ &+ \alpha_2^2 \left(z \sin^2 \varphi + \frac{1}{z} \cos^2 \varphi \right) \\ &\left. + 2\alpha_1 \alpha_2 \left(\frac{1-z^2}{z} \sin \varphi \cos \varphi \right) \right] \end{aligned} \quad (26)$$

Eq.26 can be simplified by noting that the phase shift angle φ can be absorbed without loss of generality in the vector of displacements through a rotation $R(\varphi)$:

$$\begin{pmatrix} \alpha_1 \\ \alpha_2 \end{pmatrix} = \begin{pmatrix} \cos(\varphi) & \sin(\varphi) \\ -\sin(\varphi) & \cos(\varphi) \end{pmatrix} \begin{pmatrix} \alpha'_1 \\ \alpha'_2 \end{pmatrix} \quad (27)$$

and so the uncertainty in photon number yields

$$\Delta N = \sqrt{\frac{1}{8}\nu^2 \left(z^2 + \frac{1}{z^2} \right) - \frac{1}{4} + \nu \left(\alpha_1'^2 z + \alpha_2'^2 \frac{1}{z} \right)} \quad (28)$$

and through the quotient between Eqs.25 and 28 one can compute the ratio Γ of any Gaussian state as a function of the squeezing and displacement transformations.

Optimal *signal-to-noise* ratio Γ for Gaussian states

In order to obtain the Gaussian transformation that minimizes the uncertainty in the harvested energy, constrained to a fixed temperature of the system and to some maximum amount of such energy, we apply the method of Lagrange multipliers to the following optimization problem:

Minimize

$$f(z, \alpha_1, \alpha_2) = \frac{1}{8}\nu^2 \left(z^2 + \frac{1}{z^2} \right) + \nu \left(\alpha_1^2 z + \alpha_2^2 \frac{1}{z} \right)$$

Subject to

$$g(z, \alpha_1, \alpha_2) = \frac{1}{4}\nu \left(z + \frac{1}{z} - 2 \right) + |\alpha|^2 \leq \epsilon$$

$$0 < z \leq 1$$

This strategy first provides us with the optimal Gaussian squeezing z (as a function of the two fixed parameters) in the form of an implicit quartic equation. We are interested in the solution that is a physical value of squeezing (i.e., is real and lies within the interval $(0, 1]$).

$$\nu \left(\frac{1}{z_{\text{opt}}^3} + z_{\text{opt}} - 2 \right) = 4\epsilon \quad z \in \mathbb{R}, z \in (0, 1] \quad (30)$$

According to Lagrange's equations, the optimal displacement $\vec{\alpha}$ parameters depend on the previously obtained

optimal squeezing through:

$$\begin{aligned}\alpha_{1,opt}^2 &= \frac{\nu}{4} \left(\frac{1}{z_{opt}^3} - \frac{1}{z_{opt}} \right) \\ \alpha_{2,opt}^2 &= 0\end{aligned}\quad (31)$$

and finally the optimal Gaussian ratios Γ , which are shown in Fig.2, are simply calculated by substituting these optimal solutions for z and $\vec{\alpha}$ into Eqs.25 and 28.

To get a hint on how much of each energetic resource (squeezing and displacement) contributes to the optimal Gaussian state, we show the numerical values of the solutions as a function of T, ϵ in Fig.5. Whereas the optimal displacement seems to simply increase as more energy is allowed into the system, regardless of temperature, the optimal squeezing displays a less uniform behaviour. Interestingly, for most of the (T, ϵ) values, highly squeezed states (i.e. z_{opt} small) are advantageous, and so for the majority of the parameter space we may approximate

$$\frac{1}{z_{opt}^3} \gg z_{opt} \quad (32)$$

and solve Eq.30 explicitly for the squeezing parameter:

$$z_{opt} \approx \left(\frac{4\epsilon}{\nu} + 2 \right)^{-\frac{1}{3}} \quad (33)$$

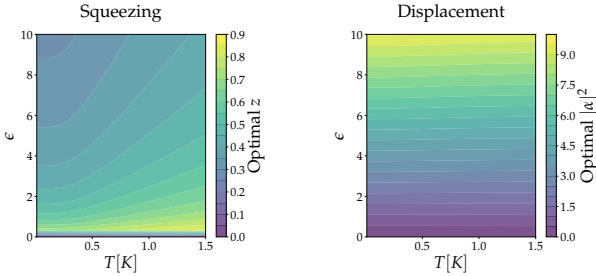


FIG. 5: Solution to 29 for the optimal squeezing and displacement through the Lagrange multipliers method.

With this approximation, the optimal Gaussian *signal-to-noise* ratio finally yields:

$$\Gamma_{opt} \approx \frac{8\epsilon}{\nu^2 \left[3 \left(\frac{4\epsilon}{\nu} + 2 \right)^{\frac{2}{3}} - 2 + \left(\frac{4\epsilon}{\nu} + 2 \right)^{-\frac{2}{3}} \right]} \quad (34)$$

Expectation values on non-Gaussian states

The procedure for computing the expectation value and uncertainty of the photon number operator to optimize our objective quantity Γ assumes that any quantum operator M can be written as a product of ladder operators, and also that the output state after the whole circuit can be written as another product of ladder operators acting

on an underlying Gaussian state with density matrix ρ_G :

$$M = \prod_{j=1}^n a_j^{\#}, \quad \rho_{NG} = \frac{1}{K} \prod_{i=1}^m a_i^{\#} \rho_G (a_i^{\#})^\dagger$$

where $\# \in \{\dagger, \cdot\}$ denotes the type of ladder operator (creation or annihilation, respectively), and $K := \text{Tr} \left[\prod_{i=1}^m a_i^{\#} \rho_G (a_i^{\#})^\dagger \right]$ is a normalization factor that comes from the fact that ladder operators are non-unitary. By the cyclic property of the trace:

$$\text{Tr} [M \rho_{NG}] = \frac{1}{K} \text{Tr} \left[a_{S_m}^\dagger \dots a_{S_1}^\dagger a_{C_n}^\# \dots a_{C_1}^\# a_{S_1} \dots a_{S_m} \rho_G \right] \quad (35)$$

where operators with subscript S_i are those implementing the photon subtractions (analogous for additions by taking hermitian conjugates) on mode i of the Gaussian state, and those with subscript C_j comprise the expression of the observable M whose expectation value we wish to calculate. From Wick's theorem we know that the expectation value of a single product of ladder operators can be decomposed as the following sum:

$$\begin{aligned}\text{Tr} \left[a_{S_m}^\dagger \dots a_{S_1}^\dagger a_{C_n}^\# \dots a_{C_1}^\# a_{S_1} \dots a_{S_m} \rho_G \right] &= \\ = \sum_{\mathcal{P}} \prod_{\{(p_1, \#), (p_2, \#)\} \in \mathcal{P}} \text{Tr} \left[a_{p_1}^\# a_{p_2}^\# \rho_G \right] &\quad (36)\end{aligned}$$

where \mathcal{P} is the set of all possible perfect matchings of the $2m+n$ indices $(p_k, \#) \in \{C_1, \dots, C_n, S_1, \dots, S_m\} \times \{\dagger, \cdot\}$ of the ladder operators, including loops (i.e. matchings of one of the operators with itself [42]). All we are left with are expectation values of singlets or pairs of annihilation or creation operators on a Gaussian state, which can be computed by using the following identities:

$$\begin{aligned}d_1 &= \text{Tr} [a_j \rho_G] = \alpha_j \\ d_2 &= \text{Tr} [a_j^\dagger \rho_G] = \alpha_j^* \\ I_1 &= \text{Tr} [a_j^\dagger a_k^\dagger \rho_G] = \frac{1}{4} [V_{jk} - V_{j+N, k+N} - i(V_{j, k+N} + V_{j+N, k})] \\ I_2 &= \text{Tr} [a_j a_k \rho_G] = I_1^* \\ I_3 &= \text{Tr} [a_j^\dagger a_k \rho_G] = \frac{1}{4} [V_{jk} + V_{j+N, k+N} + i(V_{j, k+N} - V_{j+N, k}) - 2\delta_{jk}] \\ I_4 &= \text{Tr} [a_j a_k^\dagger \rho_G] = \delta_{jk} + I_3^*\end{aligned}\quad (37)$$

where α_j and V_{jk} are the j -th mode's displacement and the (j, k) matrix element of the $2N \times 2N$ covariance matrix of the quadratures of the state ρ_G , respectively.

Example: kitten states

Cat states, defined in quantum optics as superpositions of coherent states with opposite phases, present significant challenges for experimental realization. However, it has been shown that these states can be approximated—hence the term *kitten*—by successively applying photon subtractions to a squeezed thermal

state [39, 40] (cat states would correspond to the limit of infinite subtractions). This approach not only simplifies their practical implementation but also yields a particular class of non-Gaussian distributions for which the statistical moments of the photon-number observable can be handled analytically.

Let us consider the covariance matrix of a thermal squeezed state of a single mode

$$\sigma = \begin{pmatrix} \nu z & 0 \\ 0 & \frac{\nu}{z} \end{pmatrix}$$

where ν is the noise parameter and z accounts for squeezing. Since we are not considering displacement, $\alpha = \mathbf{0}$. The Wick identities (Eq.37) for the corresponding state take the form:

$$\begin{aligned} d_1 &= d_2 = 0 \\ I_1 &= I_2 = \frac{\nu}{4} \left(z - \frac{1}{z} \right) \\ I_3 &= \frac{\nu}{4} \left(z + \frac{1}{z} \right) - \frac{1}{2} \\ I_4 &= \frac{\nu}{4} \left(z + \frac{1}{z} \right) + \frac{1}{2} \end{aligned} \quad (38)$$

Now, suppose we perform m successive photon subtractions on the previous thermal squeezed state. The mean values of the photon number and its square for the output non-Gaussian state read:

$$\begin{aligned} N_{cat} &= \frac{1}{K} \text{Tr} \left[\underbrace{a^\dagger a}_N \underbrace{a \dots a}_m \sigma \underbrace{a^\dagger \dots a^\dagger}_m \right] = \\ &= \frac{1}{K} \text{Tr} \left[\underbrace{a^\dagger \dots a^\dagger}_{m+1} \underbrace{a \dots a}_{m+1} \sigma \right] \end{aligned} \quad (39)$$

$$\begin{aligned} N_{cat}^2 &= \frac{1}{K} \text{Tr} \left[\underbrace{a^\dagger a a^\dagger a}_{N^2} \underbrace{a \dots a}_m \sigma \underbrace{a^\dagger \dots a^\dagger}_m \right] = \\ &= \frac{1}{K} \text{Tr} \left[\underbrace{a^\dagger \dots a^\dagger}_{m+1} a a^\dagger \underbrace{a \dots a}_{m+1} \sigma \right]^{[a, a^\dagger] = 1} \\ &= \frac{1}{K} \left(\text{Tr} \left[\underbrace{a^\dagger \dots a^\dagger}_{m+1} \underbrace{a \dots a}_{m+1} \sigma \right] + \text{Tr} \left[\underbrace{a^\dagger \dots a^\dagger}_{m+2} \underbrace{a \dots a}_{m+2} \sigma \right] \right) \end{aligned} \quad (40)$$

with

$$\begin{aligned} K &= \text{Tr} \left[\underbrace{a \dots a}_m \sigma \underbrace{a^\dagger \dots a^\dagger}_m \right] = \\ &= \text{Tr} \left[\underbrace{a^\dagger \dots a^\dagger}_m \underbrace{a \dots a}_m \sigma \right] \end{aligned} \quad (41)$$

By examination of Eqs. 39-41, we notice in fact we only need to calculate

$$f(r) = \text{Tr} \left[\underbrace{a^\dagger \dots a^\dagger}_r \underbrace{a \dots a}_r \sigma \right] \quad (42)$$

for some generic r , and the *signal-to-noise* ratio can be

straightforwardly be derived from it through

$$\Gamma_{cat} = \frac{N_{cat} - N_0}{\sqrt{N_{cat}^2 - (N_{cat})^2}} = \frac{\frac{f(m+1)}{f(m)} - N_0}{\sqrt{\frac{f(m+1)+f(m+2)}{f(m)} - \left(\frac{f(m+1)}{f(m)} \right)^2}} \quad (43)$$

where

$$N_0 = \frac{1}{2}(\nu - 1)$$

is the mean photon number of the initial thermal state (before applying the squeezing transformation).

Once the problem has been reduced to computing $f(r)$ using the method proposed in the previous section, we notice that the identification of perfect matchings of the ladder operators will differ depending on the parity of r . We will examine both alternatives separately.

Case r even. In this case homogeneous matchings are possible (i.e matchings that pair all of the creation operators among themselves, and all of the annihilation operators among themselves).

- The amount of different homogeneous matchings that can be done is

$$\left(\frac{r!}{2^{\frac{r}{2}} \left(\frac{r}{2}! \right)} \right)^2$$

since there exist $r!$ different permutations of r elements, but the $\left(\frac{r}{2}! \right)$ permutations of the pairs are considered identical, and so are the $2^{\frac{r}{2}}$ permutations of the two elements within each pair. The square accounts for the fact that the same logic applies to both the creation and the annihilation operators.

- If, on the contrary, we paired all of the creation operators with an annihilation one (all non-homogeneous pairs), we would have $r!$ possibilities (the first a would choose among r different a^\dagger 's, the second one among the remaining $r - 1$, etc).
- The mixed approach in this case would be to make some $a^\dagger a$ pairs (necessarily an even number $s = 2j$ of them) and mix the rest of operators homogeneously. The number of options here takes the form:

$$s! \binom{r}{s}^2 \left(\frac{(r-s)!}{2^{\frac{r-s}{2}} \left(\frac{r-s}{2}! \right)} \right)^2 \equiv b_r(s)$$

Taking into account all these possibilities and applying Eqs.36, 37, we obtain the expression:

$$f(r) = \sum_{j=0}^{\frac{r}{2}} b_r(2j) \cdot I_3^{2j} \cdot I_1^{\frac{r-2j}{2}} \cdot I_2^{\frac{r-2j}{2}} \quad \text{for } r \text{ even} \quad (44)$$

Case r odd. In this case homogeneous matchings are not possible, and an odd number of operators of each

kind have to be paired non-homogeneously. Reasoning analogously as in the even case, we are left with:

$$f(r) = \sum_{j=0}^{\frac{r-1}{2}} b_r(2j+1) \cdot I_3^{2j+1} \cdot I_1^{\frac{r-2j-1}{2}} \cdot I_2^{\frac{r-2j-1}{2}} \quad \text{for } r \text{ odd} \quad (45)$$

Note that these expressions (Eqs.44,45) can be applied to compute the mean photon number of any Gaussian non-displaced state undergoing successive photon subtractions. However, unlike the case of kitten states (where the covariance matrix of the squeezed thermal state is diagonal), the equality $I_1 = I_2$ will not necessarily hold in general.

Minimum Entropy of non-Gaussian states

The non-Gaussian states that we propose in this work as most suitable batteries for precision energy harvesting have the following structure:

$$\rho_{NG} = (a_1^\dagger)^m U_G \rho_{th}^0 U_G^\dagger (a_1)^m \quad \text{for } m = 1, 2, 3... \quad (46)$$

where m denotes their stellar rank, U_G is a general Gaussian transformation, and ρ_{th}^0 is the passive thermal state of the system given some fixed fluctuation level parametrized by a temperature T . Figure 4 shows that in principle, higher m (that is, higher non-gaussianity) results in an advantage in terms of our figure of merit Γ . However, every photon added to the system conveys an energy increase, which may result in a violation of the constraint $\delta N \leq \epsilon$, and thus in the impracticability of the resulting state for the application that was pursued. In what follows, we will derive the explicit expression for such increase.

The covariance matrix of ρ_{th}^0 is, for the single-mode case, given by

$$\sigma_{th}^0 = \begin{pmatrix} \nu & 0 \\ 0 & \nu \end{pmatrix} \quad \text{where } \nu \equiv \coth\left(\frac{\omega}{2T}\right)$$

Since ρ_{th}^0 is Gaussian, its mean photon number, which we denote N_0 , can be directly calculated through 23:

$$N_0 \equiv N(\rho_{th}^0) = \frac{1}{2}(\nu - 1)$$

And $\delta N = 0$, since the state is passive (it is the initial input state).

Adding photons to this passive thermal state naturally conveys an increase in average energy. In particular, the least possible energy that one may reach after m photon additions is that of the state $\rho_{th}^{(+m)} = a^{\dagger m} \rho_{th}^0 a^m$ (where we have dropped the indices since we are dealing with only one mode). That is, successively adding (analogous for subtracting) the m photons to ρ_{th}^0 , without previously performing any Gaussian transformations (which would

increase energy even further). The analytical derivation of the mean photon number $\langle N \rangle = \langle a^\dagger a \rangle$ for this particular class of states $\rho_{th}^{(+m)}$ appears to be particularly simple. As before, this is equivalent to computing

$$\frac{1}{K} \text{Tr}[\underbrace{a \dots a}_{m \text{ times}} \underbrace{a^\dagger a}_N \underbrace{a^\dagger \dots a^\dagger}_{m \text{ times}} \rho_{th}^0] \quad (47)$$

with

$$K = \text{Tr}[\underbrace{a \dots a}_{m \text{ times}} \underbrace{a^\dagger \dots a^\dagger}_{m \text{ times}} \rho_{th}^0] \quad (48)$$

For the identification and sum over all possible *perfect matchings* of the ladder operators, we recall the diagonal form of the covariance matrix of ρ_{th}^0 , and we realize there are only two non-zero entries:

$$V_{11} = V_{22} = \nu$$

With this, $I_1 = I_2 = 0$, $I_3 = N_0$, and $I_4 = N_0 + 1$, and we must only consider non-homogeneous perfect matchings $a^\dagger a$ or aa^\dagger . From a set of $m+1$ creations a^\dagger and $m+1$ annihilators a ordered as in Eq.47, there are only two possible configurations:

- All pairs have the annihilator to the left: there are $m \cdot m!$ possible combinations for this, but $m!$ of them cancel out with the denominator K , so we are left with

$$m \cdot \text{Tr}[aa^\dagger] = m \cdot I_4 = m(N_0 + 1)$$

- The central pair $a^\dagger a$ is fixed, and the other operators can be paired as aa^\dagger in $m!$ different ways, all $m!$ cancelled with the denominator K . In this case we have just

$$\text{Tr}[a^\dagger a] = I_3 = N_0$$

Summing up both, we finally have the analytic expression for the mean photon number N and photon number increase δN of the state of lowest energy among those with the structure of Eq.46:

$$N(\rho_{th}^{(+m)}) = m(N_0 + 1) + N_0 \quad (49)$$

$$\delta N(\rho_{th}^{(+m)}) = m(N_0 + 1) = m \frac{\coth\left(\frac{1}{2T}\right) + 1}{2} \quad (50)$$

Therefore, the existence of a constraint ϵ in the maximum photon number input means we cannot apply as many photon additions as we want, but instead a maximum amount given by the expression:

$$m_{max} = \left\lfloor \frac{2\epsilon}{\coth\left(\frac{1}{2T}\right) + 1} \right\rfloor \quad (51)$$

If some specific use-case has a very restrictive constraint ϵ on the maximum energetic input, the maximum

allowed m may be zero and so the correct charging unitary to use in our application can only be a Gaussian one. In Fig.6 one can see the optimal Γ attainable with zero, one, two, and three photon-added states, as a function of the ergotropic constraint. Temperature has been set to $T = 0.5K$ arbitrarily. Non-Gaussian

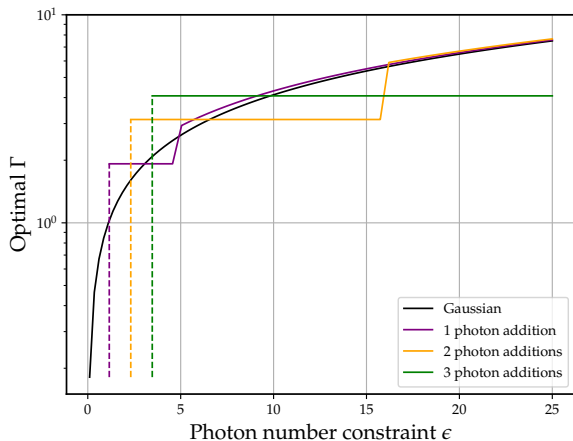


FIG. 6: Optimal Γ for Gaussian and non-gaussian photon-added single-mode states as a function of the constraint ϵ , at fixed temperature $T = 0.5K$

states are dominant from the initial region (where only Gaussian ones are feasible) onwards. However, one can identify an interval in which the Gaussian bound is widely violated by some photon-added state, while as the constraint is relaxed, the gain becomes close to negligible. This is consistent with the fact that, without the energetic restriction, one can achieve as high Γ as desired just by applying displacement operations, which fall within the Gaussian realm.

Effects of truncation

Despite the simplicity of the two particular cases outlined above, the exact calculations of expectation values on non-Gaussian states are, in general, computationally resource-demanding. They scale as $N!!$ with the number N of ladder operators involved, counting both those included in the operator whose expectation value we are computing, and those applied to construct the non-Gaussian distribution. However, typical approaches to this exact calculation (i.e., discrete-variable approximations made by truncating the dimension of the Hilbert space) can lead to misleading and unfair conclusions, as we are about to show. We will proceed by proving that truncating the Hilbert space of a coherent state $|\alpha\rangle$, allows the violation of the Gaussian bound.

Let us consider the Fock basis of a finite-dimensional Hilbert space with truncation to the second excited state: $\mathcal{H} = \text{span}(\{|0\rangle, |1\rangle, |2\rangle\})$. Then the definition of $|\alpha\rangle$

would be approximated to $|\alpha\rangle_t$ in the following way:

$$|\alpha\rangle = \sum_n \frac{\alpha^n}{n!} e^{-\frac{|\alpha|^2}{2}} |n\rangle \approx \approx |\alpha\rangle_t \equiv C \left(|0\rangle + \frac{\alpha}{\sqrt{1!}} |1\rangle + \frac{\alpha^2}{\sqrt{2!}} |2\rangle \right) \quad (52)$$

where C is a normalization factor required to make up for the lost probabilities:

$$C = \left(1 + |\alpha|^2 + \frac{|\alpha|^4}{2} \right)^{-1/2}. \quad (53)$$

Then, the photon number expectation value and uncertainty on $|\alpha\rangle_t$ yield:

$$\Gamma(|\alpha\rangle_t) = \frac{\langle N \rangle}{\Delta N} = \frac{C^2 (|\alpha|^2 + |\alpha|^4)}{\sqrt{C^2 (|\alpha|^2 + 2|\alpha|^4) - C^4 (|\alpha|^2 + |\alpha|^4)^2}} \quad (54)$$

which can be shown to be always greater than $|\alpha|$, which is the existing bound on Γ for coherent states, as shown in Eq.12. In other words, by a mere approximation, we gain a non-classical resource in terms of charging precision. Obviously, by increasing the dimension of the Hilbert space enough, we should recover the correct result. However, this would make the calculations more tedious than the exact result we provide, employing the Wick theorem.

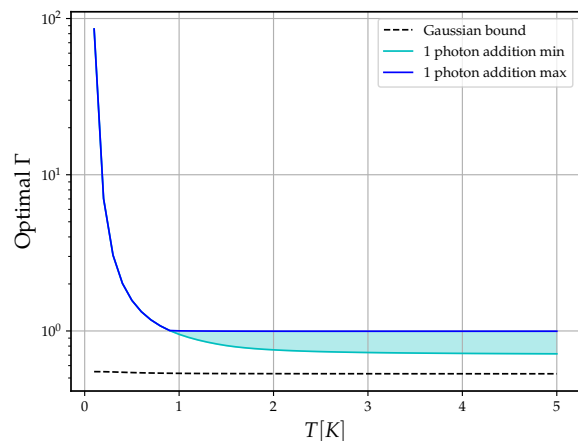


FIG. 7: Optimal *signal-to-noise* ratio for Gaussian, one-photon added separable and one-photon added entangled states of two modes, as a function of system's temperature. The energetic constraint has been set as $\sum_{i=1,2} \delta N_i \leq \epsilon = 5$

Multimode case

When the battery system comprises multiple modes, the possibility to perform entangling operations between them is unlocked. This naturally raises the question of whether such operations can offer an advantage in the relative precision of the stored energy. In the most

general case, each of the modes may have different oscillating frequencies, and a comment in this regard is made in [34] on the fact that Gaussian passive optics are sufficient to mix the modes in such a way that photons are stored in the lower frequency modes, implying a gain in energy precision.

However, in our scenario the response of the harvester is uniquely dependent on the photon number statistics (thus equivalent to the case where the battery modes all oscillate at the same frequency ω). In that case, it can be shown that through Gaussian global (entangling) unitaries only, our figure of merit Γ remains constant. On the contrary, non-Gaussian states feature *signal-to-noise ratios* that are tunable by passive, entangling operations, allowing for some extra advantage with respect to the Gaussian case when the correct beam-splitting angle is applied. In this sense, our figure-of-merit constitutes a signature of non-Gaussianity, because the dependency of Γ on the parameters of an entangling operation, such as a beam splitter, is an exclusive property of non-Gaussian states. In Fig.7 we show the value of Γ for the optimal

two-mode one-photon added state, both in the separable case (yielding the worst ratio) and the maximally entangled one. The shaded area represents the gain given by the application of a $\theta = \pi/4$ beam splitter. Note that, for low temperatures, entanglement plays no role since, as mentioned above, close to the pure state regime, Fock states are always optimal in terms of photon number uncertainty. Finally, we address the question of whether this advantage is extensive with the number of modes. In Fig.8 we show the optimal *signal-to-noise* ratio Γ (upon tuning of the squeezing, beam-splitting, phase-shifting and displacement parameters) attainable for multimode batteries of increasing degrees of non-Gaussianity. From the results, we conclude that the hierarchy in extractable *signal-to-noise* ratios established by the degree of non-Gaussianity in the single mode case is a property that can be generalized to larger N , and the existent increasing trend of Γ with N suggests that bigger and more complex non-gaussian battery systems hold a promising potential as highly precise energy storage devices.

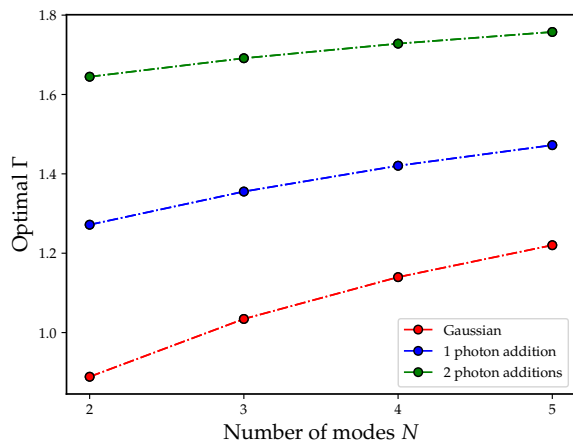


FIG. 8: Optimal *signal-to-noise* ratio for Gaussian, one-photon added and two-photon added entangled states as a function of the number of modes $N \in \{2, 3, 4, 5\}$. System's temperature and energetic constraint have been set at $T = 0.5K$ and $\sum_i \delta N_i \leq \epsilon = 10$, respectively.